Robust Approach for Butterfly Species Classification Using A Single Spatio-Hyperspectral Image

Erick Adje, Gilles Delmaire, Arnaud Ahouandjinou, Matthieu Puigt, Gilles Roussel

ROBUST APPROACH FOR BUTTERFLY SPECIES CLASSIFICATION USING A SINGLE SPATIO-HYPERSPECTRAL IMAGE

Erick A. Adjé[1,2], *Gilles Delmaire*[1], *Arnaud S. R. M. Ahouandjinou*[2], *Matthieu Puigt*[1], *and Gilles Roussel*[1]

[1]*Univ. Littoral Côte d'Opale, LISIC – UR 4491*, F-62219 Longuenesse, France
[2]*Univ. d'Abomey-Calavi, LRSIA*, Cotonou, Benin

ABSTRACT

Distinguishing between pest and pollinator butterfly species is a major challenge in precision agriculture. However, traditional RGB cameras, capturing only shape and surface color, are insufficient for detailed insect analysis. This work explores the rich spectral information provided by hyperspectral imaging for effective butterfly species identification. For this purpose, we use a single spatio-spectral image that provides partial spectral information to identify the butterfly species. The proposed classification approach consists of a convex combination of the probabilistic decisions obtained by the Gaussian Naive Bayes and Z-score methods for each butterfly reflectance. Compared to traditional classification models, this approach showed higher robustness and performance.

Index Terms— Precision agriculture, Hyperspectral Imaging, Spatio-spectral camera, Butterfly recognition, Gaussian mixture models

1. INTRODUCTION

Butterflies are crucial in maintaining the balance of ecosystems. While some species significantly contribute to pollination and biodiversity, others pose substantial threats by laying eggs on plant leaves, leading to larvae that devastate crops. Unfortunately, control methods are often deployed too late, after damage has already begun, resulting in the hazard use of harmful pesticides and an estimated 20-40% annual loss in global agricultural production [1]. An effective approach would involve taking preventive measures when pest butterflies are detected to prevent them from laying eggs. The success of such an approach depends on having a robust detection system that distinguishes pest butterflies from pollinators. With recent advances in precision agriculture, several butterfly species recognition systems based on conventional RGB cameras have emerged. Using traditional machine learning techniques, models are built from various features extracted from labeled butterfly images. Texture and pattern features are typically derived using methods like Gray Level Co-occurrence Matrix (GLCM) and Local Binary Pattern (LBP). These features are then used to train algorithms such as K-Nearest Neighbours (K-NN) [2], Support Vector Machine (SVM) [3] and Multinomial Logistic Regression (MLR) [4] for butterfly species recognition. In addition, advanced deep learning methods such as YOLO [5] and AlexNet [6] have been explored on large datasets of over 80 butterfly species. However, a study shows that RGB cameras have limitations because they only capture surface color with three channels, which may not accurately reflect the complex characteristics of insects [7]. Therefore, our study investigates the use of Hyperspectral Imaging (HSI) for butterfly species recognition. HSI generates a 3D hyperspectral datacube with two spatial dimensions and one wavelength dimension, allowing analysis on over 100 wavelengths, unlike Multispectral Imaging (MSI) which processes far fewer than 100 wavelengths. Among them, MSI snapshot cameras have limited spectral resolution and require demosaicing steps [8] while CASSI HSI cameras [9] are not commercially available. We then choose a specific spatio-spectral camera owing to its high spectral resolution, enable to distinguish between species with similar color patterns and detect them in complex vegetation environments.

However, to the best of our knowledge, no study has used HSI for butterfly species classification. Existing research focuses only on the spectral analysis of their wing structure [10, 11]. From our side, our first proposed approach [12] uses a spatio-spectral camera for butterfly species classification, applying Gaussian Naive Bayes and Z-score methods for pixel voting. However, this binary decision strategy was too strict, as it ignores significant trends toward multiple species, favoring the dominant one and eliminating the doubt between similar species. In this paper, we propose a more robust approach for butterfly species classification using a single raw image from a compact spatio-spectral camera. The challenge with a spatio-spectral camera lies in the necessity of a complete scan to capture an object across all spectral strips, followed by datacube reconstruction [13]. This process is time-consuming and impractical for real-time tasks like early detection of crop-damaging butterflies. The work presented in this paper is the initial phase of a new research that introduces an unconventional use of the spatio-spectral camera for real-time detection of pest butterflies. The approach involves set-

E. A. Adjé thanks IITA Benin for the PhD co-funding.

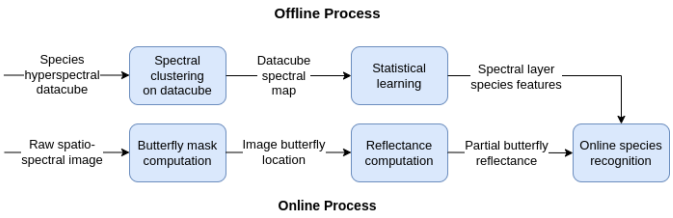

Fig. 1. General methodology of the classification process

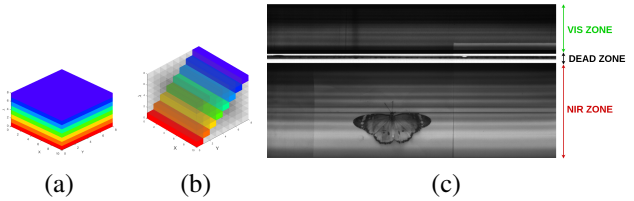

Fig. 2. HSI content of (a) Conventional, (b) Spatio-spectral camera. (c) Raw spatio-spectral image

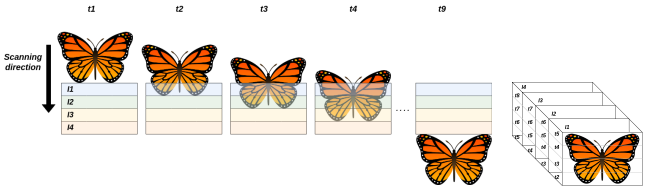

Fig. 3. HSI cube formation using a spatio-spectral Camera

ting up a stationary camera to monitor a vegetation-covered field. Then, the random movement of butterflies across the camera spectral layers provides partial spectral data used to recognize the species in real-time, without needing datacube reconstruction. The real-time recognition is based on a prior species characterization step performed offline. Here, the preliminary task focuses on identifying the species of a stationary butterfly detected in a limited number of spectral layers within a single raw image.

The general scheme is described in Fig 1 and the paper is organized as follows: Sec. 2 describes the camera and data collection. Sec. 3 outlines the proposed methodology. Sec. 4 presents the results and comparisons with existing methods.

2. DATA COLLECTION

2.1. Spatio-spectral Camera Description

The camera employed in the present study is a compact hyperspectral camera designed for industrial applications, specifically the *XIMEA xiQ MQ022HG-IM-LS150 VISNIR* model. With a high resolution, it covers a spectral range of 470-900 nm, which provides images in both the visible (VIS) and near-infrared (NIR) spectrum. The camera, equipped with the *IMEC CMV2K-LS150* sensor model, incorporates a Fabry-Perot filter array that captures 192 spectral profiles. Fig. 2-c shows a typical raw image structure whose effective area is 960×2048 pixels, with 192 spectral strips, each 5 pixels wide. Unlike traditional hyperspectral cameras, which provide a complete spectral cube (see Fig. 2-a), the spatio-spectral camera offers only a staircase-like portion, as shown in Fig. 2-b. Because a single camera capture provides partial spectral content, a full scan of the specimen across all spectral strips is required to build a complete cube. To achieve this, strips of the same wavelength from the partial images are rearranged across successive frames, followed by heavy additional processing to ensure a high-quality hyperspectral cube [13] (see Fig. 3). This process generates 192 2D spectral images which are sequentially concatenated to form the hyperspectral datacube.

2.2. Butterfly Species

This paper focuses on four butterfly species : *Hypolimnas Misippus* (HM), *Danaus Chrysippus* (DC), *Amauris Ochlea* (AO), and *Acraea Egina* (AE) belonging to the Nymphalidae family. In their butterfly stage, they mainly act as pollinators. However, an overabundance of these species could result in crop damage. These species were captured and studied in a citrus field at the International Institute of Tropical Agriculture (IITA) of Benin. Data collection of these species was performed in two stages. The first involved full scans of different specimens for each species to build complete hyperspectral cubes which were used for characterization of the species. The second stage was to acquire single images of different specimens, resulting in a dataset of raw spatio-spectral images on which our classification approach was applied.

3. PROPOSED METHODOLOGY

3.1. Species Characterization

Firstly, we identify the similar spectral regions within the complete hyperspectral cubes of each species. For this purpose, we used the K-means method to cluster similar spectra for each species. However, selecting the appropriate number of clusters, K^u for each species $u \in \{HM, DC, AO, AE\} \triangleq \{1, 2, 3, 4\}$ can significantly affect the performance. A minimal number of clusters can result in overlapping features between species, while a huge number can result in features that are unrepresentative of the species. Based on some empirical experiences and the using of the Elbow Curve method, the best K^u values found are: $K^{HM} = 3$, $K^{DC} = 4$, $K^{AO} = 4$ and $K^{AE} = 3$, respectively for species HM,

DC, AO and AE. Fig. 4 presents the similar spectral regions for each species. Let $\underline{s}_i = [r_i^1, r_i^2, ...r_i^{192}]^T$, the spectrum of pixel p_i in any hyperspectral cube, where r_i^b is the reflectance of a spectral layer $b \in \{1, \ldots, 192\}$ of p_i. The clustering step of similar spectra produced the set of spectra $G^{(u,k)}$ for cluster $k \in \mathcal{K} \triangleq \{1, \ldots, K^u\}$ from each species u. Let $\mathcal{I}^{(u,k)} \triangleq \{i \in \mathbb{N} \text{ s.t. } \underline{s}_i^u \in \text{Cluster } k\}$ the set of indices of extended pixels indices that belong to Cluster k. $G^{(u,k)}$ is defined such that $\forall\, i \in \{1, \ldots, \#\mathcal{I}^{(u,k)}\}$, $G^{(u,k)}(i) \triangleq \underline{s}_{\mathcal{I}^{(u,k)}(i)}$. Then, we assume that for any species u, the reflectance values within the same spectral layer b in cluster k are modeled by a random variable that follows a Gaussian distribution denoted as $\mathcal{N}(\mu_b^{(u,k)}, \sigma_b^{(u,k)})$ whose parameters depend on the band number. Each Gaussian distribution is identified using the $n^{(u,k)}$ reflectance values $G^{(u,k)}(b,:) = [G^{(u,k)}(b,1) \ldots G^{(u,k)}(b, n^{(u,k)})]$. To estimate the parameters of the Gaussian distributions, we assume that the identified spectral regions within each species have equal probabilities of occurrence. Thus, for a cluster k of a species u, we get the 2 x 192 matrix $M^{(u,k)}$ and its extension M^u to the K^u clusters of species u: $M^u = [{M^{(u,1)}}^T \ldots {M^{(u,K^u)}}^T]^T$. Our species characterization step corresponds to a Gaussian Mixture Model with 14 classes per spectral layer (3 classes for HM, 4 classes for DC and AO, and 3 classes for AE).

$$M^{(u,k)} = \begin{bmatrix} \mu_1^{(u,k)} & \mu_2^{(u,k)} & \ldots & \mu_{192}^{(u,k)} \\ \sigma_1^{(u,k)} & \sigma_2^{(u,k)} & \ldots & \sigma_{192}^{(u,k)} \end{bmatrix} \tag{1}$$

3.2. Extraction of Butterfly Reflectances

To extract butterfly reflectances from a raw spatio-spectral image $I(x,y)$, we first compute the mask $Mask(x,y)$ through normalization and background subtraction using a reference image, as shown in Fig. 5. The mask is then split into spectral layers: $Mask(x,y,b)$, $b \in \{1, \ldots, 192\}$ but we retain only the $Mask(x,y,b^*)$ of spectral layers b^* where the butterfly was detected with $b^* \in \mathcal{B}^*$ and $\mathcal{B}^*$ the set of detection layers. For each detection pixel $p_{b^*}^i$ in b^*, reflectance $r_{b^*}^i$ is evaluated using the part of spectralon in the same layer, producing the reflectance vector $\underline{r}_{b^*} = \left[r_{b^*}^1, \quad r_{b^*}^2, \ldots (r^{n^{b^*}})_{b^*}\right]^T$, where n^{b^*} is the pixel number in layer b^* where the butterfly is present.

3.3. Classification strategy of the butterfly species

Based on $b^* \in \mathcal{B}^*$, we extract the parameters $(\mu_{b^*}^{(u,k)}, \sigma_{b^*}^{(u,k)})$, $\forall\, k \in \{1, \ldots, K^u\}$ of b^*, from the Gaussian distributions obtained in the characterization phase of each species. Then, we try to assign each reflectance $r_{b^*}^i$, of the butterfly to one of the extracted distribution according to b^*. Some studies explore either Gaussian Naive Bayes (GNB) alone [14], or Z-Score (ZS) indexes [15], but none use both indexes. Practically, we

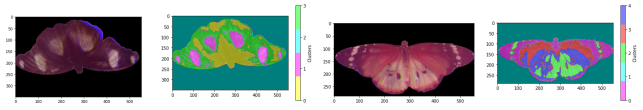

(a) HM (b) HM clusters (c) DC (d) DC clusters

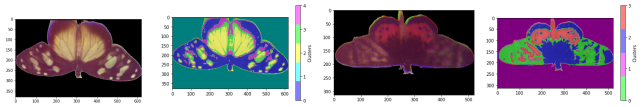

(e) AO (f) AO clusters (g) AE (h) AE clusters

Fig. 4. Clustering of Similar Spectra for Each Species

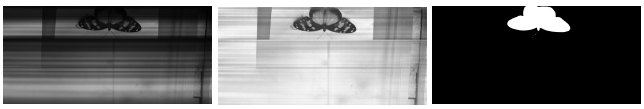

(a) Raw image (b) Normalization (c) Butterfly mask

Fig. 5. Butterfly mask computation

noticed that GNB and ZS decisions may diverge due to overlapping Gaussians caused by spectral similarities between the species. Then, it is crucial to propose a robust strategy to deal with Gaussian overlaps to predict the corresponding species in the raw image. Let denote $\Theta_{b^*}^{(u,k)} \triangleq (\mu_{b^*}^{(u,k)}, \sigma_{b^*}^{(u,k)})$. In our context, GNB uses the Naive Bayes conditional probability to identify the most probable distribution for a given reflectance $r_{b^*}^i \in \underline{r}_{b^*}$. Eq. 2 enables to calculate the set of posterior probabilities $p(u = u_i, k = k_i | r_{b^*}^i)$ according to species u and cluster k, knowing $r_{b^*}^i$. It relies on the univariate Gaussian probability density function $f(r_{b^*}^i, \Theta_{b^*}^{(u,k)})$ of the variables $r_{b^*}^i$ and $\Theta_{b^*}^{(u,k)}$ while $\pi_{u,k}$ accounts for the prior probability that $r_{b^*}^i$ belongs to Species u and cluster k. Since we assume equal probabilities for the 14 Gaussian distributions as mentioned in Subsect. 3.1, $\forall\, u \in \{1,2,3,4\}$, $\forall\, k \in \{1, \ldots, K^u\}$, $\pi_{u,k} = 1/14$. ZS consists of finding the closest distribution to $r_{b^*}^i$ using the distance defined in Eq. 3.

$$p(u = u_i, k = k_i | r_{b^*}^i) = \frac{\pi_{u,k} \cdot f(r_{b^*}^i, \Theta_{b^*}^{(u,k)})}{\sum_{u=1}^{4} \sum_{k=1}^{K^u} \pi_{u,k} \cdot f(r_{b^*}^i, \Theta_{b^*}^{(u,k)})} \tag{2}$$

$$z(u = u_i, k = k_i, r_{b^*}^i) = \frac{|r_{b^*}^i - \mu_{b^*}^{(u,k)}|}{\sigma_{b^*}^{(u,k)}} \tag{3}$$

In [12], the classification strategy we proposed, named Voting Pixel-based Detection for Global Image (VPG), involves propagating and combining the votes of each $r_{b^*}^i$ obtained with the GNB and ZS, unlike the new strategy, which propagates confidence indexes. To address this, we propose a convex combination of GNB and ZS decisions. First, we estimate the four probabilities $p(u = u_i | r_{b^*}^i)$ of each reflectance $r_{b^*}^i$ belonging to a species u using GNB. They result from

the marginalization over $k \in \{1, \ldots, K^u\}$ of the conditional probability to belong to one of the clusters k from species u, $p(u = u_i|r^i_{b^*}) = \sum_{k=1}^{K^u} p(u = u_i, k = k_i|r^i_{b^*})$. We propose here to introduce a log-likelihood index for each species u defined as : $p^u \triangleq \sum_{b^*}^{\mathcal{B}^*} \sum_{i=1}^{n^{b^*}} \log(p(u = u_i|r^i_{b^*}))$. This produces the likelihood vector describing the GNB decisions for each species defined by $\underline{p} \triangleq [p^1, p^2, p^3, p^4]$. Secondly, using the ZS index, we compute the distance $z(u = u_i, r^i_{b^*})$ of $r^i_{b^*}$ belonging to a species u, which is the minimum absolute ZS $z(u = u_i, k = k_i, r^i_{b^*})$ obtained across the various clusters $k \in \{1, \ldots, K^u\}$ of a specific species u with $z(u = u_i, r^i_{b^*}) = \underset{k=1,..,K^u}{\arg\min}\, z(u = u_i, k = k_i, r^i_{b^*})$. Subsequently, we can generate a cumulative similarity distance $z^u = \sum_{b^*}^{\mathcal{B}^*} \sum_{i=1}^{n^{b^*}} z(u = u_i, r^i_{b^*})$ for each species u. This results in the cumulative similarity distance vector $\underline{z} \triangleq [z^1, z^2, z^3, z^4]$.

Finally, a convex combination of the likelihood vector $\underline{p}$ weighted by $\alpha \in [0, 1]$ and the cumulative similarity distance $\underline{z}$ weighted by $1 - \alpha$ is performed. This involves normalizing each element of $\underline{p}$ and $\underline{z}$ by its original vector sum before performing the convex combination. Let's denote this approach : Probabilistic Pixel-based Detection for Global Image (PPG). The combination result is a decision vector $\underline{c}_{PPG}(\alpha)$ (see Eq. (4)), where the index of the smallest value represents the corresponding species u_{PPG} in the spatio-spectral image with $u_{PPG} = \underset{u=1,..,4}{\arg\min}\, \underline{c}_{PPG}(\alpha)$.

$$\underline{c}_{PPG}(\alpha) = \alpha \frac{\underline{p}}{\sum_{u=1}^{4} p^u} + (1 - \alpha) \frac{\underline{z}}{\sum_{u=1}^{4} z^u} \qquad (4)$$

4. RESULTS AND DISCUSSIONS

First, we introduce a preliminary step to determine the best α on each spectral zone. To achieve this, we implement a new phase focused on identifying the α value that gives the best performance on a training dataset composed of 176 spatio-spectral images with 88 detection images in the VIS and 88 in the NIR. The accuracy trends are then obtained on the training dataset, using a learning rate of $\alpha_{lr} = 0.02$, with $\alpha \in [0; 1]$. By replacing the best α obtained per spectral zone in Eq. (4), the decision vector $\underline{c}_{PPG}(0.84)$ will be used for the detection images in VIS area and $\underline{c}_{PPG}(0.92)$ for the detection in NIR area. To evaluate our classification strategy using the best alpha values, we apply it on an independent test dataset. This dataset consists of 160 raw spatio-spectral images, composed of 40 images per species, with 20 detection images in each spectral range (VIS and NIR). Generally, the butterfly is detected in 30 to 40 consecutive spectral strips. Tab. 1 shows the confusion matrix obtained from the test data. The results indicate that the proposed PPG strategy, which involves a convex combination, produces better results than both GNB-PPG ($\alpha = 1$) and ZS-PPG ($\alpha = 0$). These latter approaches correspond to decisions based exclusively on GNB and ZS, according to Eq. (4). Our classification strategy also performs better than the approach previously proposed in [12], as well as strategies based on traditional classification models used on RGB images, such as KNN [2], SVM [3] and MLR [4]. As deep learning approaches require large amounts of data—which are difficult to obtain—to achieve good performance, we do not explore them in this work. Our approach also shows the advantage of propagating confidence indexes of each butterfly pixel, rather than making binary decisions for each pixel. The high performance of the butterfly detection images in the NIR spectrum highlights the relevance of the hyperspectral camera in our study. The results also indicate some confusion between the DC and AO species. This confusion comes from the overlap of some Gaussian distributions during the species characterization phase owing to spectral similarities. Since there is a strong correlation between closely related spectral layers, this overlap can occur over several successive layers. To evaluate the robustness to noise of the PPG strategy compared to the VPG strategy proposed in [12], we performed a new experiment on our test data. We add different levels of Gaussian noise on the reflectance vectors $\underline{r}_{b^*}$ measured through the Signal to Noise Ratio (SNR) and evaluate the performance of both strategies. This experiment is designed to simulate the noise generated by the camera when its internal temperature rises significantly. Results presented in Fig. 6-a show better robustness of PPG compared to VPG over all noise levels. Furthermore, PPG reaches its best performance more quickly at around 35 dB, whereas VPG achieves it at 40 dB. The robustness on images of each spectral detection zone is also evaluated using the PPG strategy, as depicted in Fig. 6-b. It appears that the detection images in NIR show greater robustness regardless of the noise level. This further highlights the high discriminative potential provided by the NIR wavelengths.

Table 1. Confusion matrix obtained with PPG vs others

	Result of all samples				Result of samples in VIS				Result of samples in NIR			
Target / Predict	***HM***	***DC***	***AO***	***AE***	***HM***	***DC***	***AO***	***AE***	***HM***	***DC***	***AO***	***AE***
HM	38	2	3	8	20	2	3	8	18	0	0	0
DC	0	27	9	5	0	7	2	5	0	20	7	0
AO	0	9	28	3	0	9	15	3	0	0	13	0
AE	2	2	0	24	0	2	0	4	2	0	0	20
Sum (% good pred)	38/40 (95)	27/40 (67.50)	28/40 (70)	24/40 (60)	20/20 (100)	7/20 (35)	15/20 (75)	4/20 (20)	18/20 (90)	20/20 (100)	13/20 (65)	20/20 (100)
PPG	**Accuracy : 117/160 (73.12 %)**				**Accuracy : 46/80 (57.50 %)**				**Accuracy : 71/80 (88.75 %)**			
GNB-PPG [14]	Accuracy : 113/160 (70.62 %)				Accuracy : 44/80 (55 %)				Accuracy : 69/80 (86.25 %)			
ZS-PPG [15]	Accuracy : 89/160 (55.62 %)				Accuracy : 28/80 (35 %)				Accuracy : 61/80 (76.25 %)			
VPG [12]	Accuracy : 104/160 (65 %)				Accuracy : 39/80 (48.75 %)				Accuracy : 65/80 (81.25 %)			
KNN-VPG [2]	Accuracy : 75/160 (46.87 %)				Accuracy : 39/80 (48.75 %)				Accuracy : 36/80 (45 %)			
MLR-VPG [4]	Accuracy : 47/160 (29.37 %)				Accuracy : 27/80 (33.75 %)				Accuracy : 20/80 (25 %)			
SVM-VPG [3]	Accuracy : 44/160 (27.5 %)				Accuracy : 23/80 (28.75 %)				Accuracy : 21/80 (26.25 %)			

5. CONCLUSION

Exploring HSI for butterfly species recognition holds great potential. In this study, we propose a robust approach for butterfly species recognition based on partial spectral information from a single raw image. Unlike our previous method [12] which was based on propagating pixel decisions, we pro-

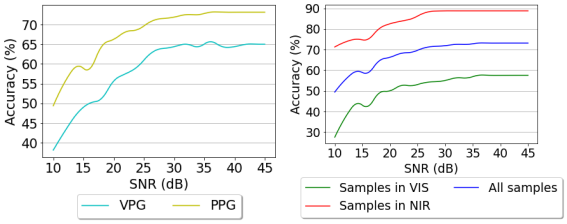

(a) PPG vs. VPG (b) PPG for each spectral zone

Fig. 6. Accuracy given multiple SNR on test data

pose here a global method based on a convex combination of global probabilistic indexes and global z-scores. This method has proven robust in the presence of overlapping Gaussian distributions caused by spectral similarities between species in certain spectral layers. An additional advantage of using a hyperspectral camera with more than a hundred spectral bands for recognition is that, even if certain species have spectral similarities that cause Gaussian overlap in several bands, there is still an opportunity to find spectral distinctions in a few bands. Our method also outperforms some state-of-the-art machine learning models used on RGB images. Future work will focus on recognizing butterflies in free flight within their natural habitats using tracking methods [16]. Our database will also be expanded with new data and species to evaluate our approach's generalization capability and the effectiveness of a deep learning approach on raw spatio-spectral images.

6. REFERENCES

[1] FAO, "International year of plant health," 2020, Accessed on 14th June, 2024.

[2] F. Li and Y. Xiong, "Automatic identification of butterfly species based on HoMSC and GLCMoIB," *The Visual Computer*, vol. 34, no. 11, pp. 1525–1533, 2018.

[3] D. S. Y. Kartika, D. Herumurti, and A. Yuniarti, "Local binary pattern method and feature shape extraction for detecting butterfly image," *GEOMATE Journal*, vol. 15, no. 50, pp. 127–133, 2018.

[4] L. Kayci and Y. Kaya, "A vision system for automatic identification of butterfly species using a grey-level co-occurrence matrix and multinomial logistic regression," *Zool. Middle East*, vol. 60, no. 1, pp. 57–64, 2014.

[5] B. Liang, S. Wu, K. Xu, and J. Hao, "Butterfly detection and classification based on integrated YOLO algorithm," in *Genetic and Evolutionary Computing*. 2020, pp. 500–512, Springer Singapore.

[6] A. Fadlil, A. Maftukhah, T. Sutikno, et al., "Butterfly image identification using multilevel thresholding segmentation and convolutional neural network classification with AlexNet architecture," *Int. J. Comput. Digit. Syst*, vol. 15, no. 1, pp. 1–9, 2024.

[7] V. Lacotte, E. Dell'Aglio, S. Peignier, et al., "A comparative study revealed hyperspectral imaging as a potential standardized tool for the analysis of cuticle tanning over insect development," *Heliyon*, vol. 9, no. 3, pp. e13962, 2023.

[8] K. Abbas, M. Puigt, G. Delmaire, and G. Roussel, "Filtering-based endmember identification method for snapshot spectral images," in *Proc. IEEE WHISPERS'22*, 2022, pp. 1–5.

[9] G. R. Arce, D. J. Brady, L. Carin, H. Arguello, and D. S. Kittle, "Compressive coded aperture spectral imaging: An introduction," *IEEE Signal Process. Mag.*, vol. 31, no. 1, pp. 105–115, 2014.

[10] B. D. Wilts, P. Pirih, and D. G. Stavenga, "Spectral reflectance properties of iridescent pierid butterfly wings," *Journal of Comparative Physiology A*, vol. 197, pp. 693–702, 2011.

[11] J. M. Medina, J. A. Díaz, E. Valero, J. L. Nieves, and P. Vukusic, "Detailed experimental characterization of reflectance spectra of sasakia charonda butterfly using multispectral optical imaging," *Optical Engineering*, vol. 53, no. 3, pp. 033111–033111, 2014.

[12] E. Adje, G. Delmaire, A. Ahouandjinou, M. Puigt, and G. Roussel, "Towards Automatic Butterfly Species Recognition Using a Single Spatio-Hyperspectral Image," in *Proc. IEEE EUSIPCO'24*, 2024, Accepted.

[13] P. Chatelain, G. Delmaire, A. Alboody, M. Puigt, and G. Roussel, "Semi-automatic spectral image stitching for a compact hybrid linescan hyperspectral camera towards near field remote monitoring of potato crop leaves," *Sensors*, vol. 21, no. 22, pp. 7616, 2021.

[14] W. Castro, M. D. la Torre, H. Avila-George, J. Torres-Jimenez, A. Guivin, and B. Acevedo-Juárez, "Amazonian cacao-clone nibs discrimination using NIR spectroscopy coupled to Naive Bayes classifier and a new waveband selection approach," *Spectrochimica Acta Part A: Molecular and Biomolecular Spectroscopy*, vol. 270, pp. 120815, 2022.

[15] I. Parshakov, C. Coburn, and K. Staenz, "Z-score distance: A spectral matching technique for automatic class labelling in unsupervised classification," in *IEEE Geosci. and Remote Sens. Symp.*, 2014, pp. 1793–1796.

[16] E. A. Adje, A. S. R. M. Ahouandjinou, et al., "Advancements in video-based insect tracking: A bibliometric analysis to a short survey," in *proc. ICAIP '23*, New York, NY, USA, 2024, p. 75–82, ACM.